# Effects of Nb Content and Thermal History on the Mechanical and Corrosion Characteristics of Stainless Steels

**Han-Cheol Choe and Kwan-Hyu Kim***

*Department of Dental Materials, School of Dentistry*
*Chosun University, Gwangju, 501-759, Korea*
**Department of Metallurgical Engineering*
*Chonnam National University, Gwangju, 500-757, Korea*

Due to excellent corrosion resistance and mechanical properties, austenitic stainless steel is widely used as the material for chemical plants, nuclear power plants, and food processing facilities. But, the zone affected by heat in the range of 400 to 800℃ during welding loses corrosion resistance and tensile strength since Cr-carbide precipitation like $Cr_{23}C_6$ forms at the grain boundary and thereby takes place the intergranular corrosion. In this study, AISI 304 stainless steel with the added Nb of 0.3 to 0.7 wt% was solutionized at 1050℃ and sensitized at 650℃. Specimen was welded by MIG. The phase and the microstructure of the specimens were examined by an optical microscope, a scanning electron microscope, and a x-ray diffractometer. The corrosion characteristics of specimens were tested by electrolytic etching and by double loop electrochemical potentiokinetic reactivation method(EPR) in the mixed solution of 0.5M $H_2SO_4$ + 0.01M KSCN.

The melting zone had dendritic structure constituted of austenitic phase and δ-ferrite phase. Cr carbide at the matrix did not appear, as Nb content increased. At the grain boundaries of the heat affected zone, the precipitates decreased and the twins appeared. The hardness increased, as Nb content increased. The hardness was highest in the order of the heat affected zone> melted zone> matrix. According to EPR curve, as the Nb content decreased, the reactivation current density(Ir) and the activation current density(Ia) were highest in the order of the melted zone<the matrix<the heat affected zone, and the grain boundaries severely corroded at the heat affected zone in the case of low Nb content.

***Keywords*** : *austenitic stainless steel, Cr-carbide, intergranular corrosion, electrochemical potentio-kinetic reactivation method(EPR), Nb content*

## 1. Introduction

Austenitic stainless steel is in growing demand thanks to its superior corrosion resistance and mechanical properties, especially for application to chemical plants, nuclear power plants, and food process equipments. But, it is supposed to have intergranular corrosion when heat-affected during processing like welding in fabricating hot water tanks or other equipments. The intergranular corrosion is cause of IGSCC (intergranular stress corrosion cracking)[1-2] and TGSCC (transgranular stress corrosion cracking)[3-4] under stress, resulting in lower corrosion resistance and mechanical properties. What affects the corrosion resistance of the sensitized stainless steel is carbon, which forms mainly $M_{23}C_6$ carbides in grain boundaries. It also forms the chrome-depleted zone,[5] which is sensitive to corrosion in grain boundaries. Many studies for prevention of the corrosion have been done. Especially, the storage tanks or heat exchangers of nuclear power plants, which are under stress, are used to get the crack initiation on the spots where the corrosion takes place. So, the studies[6-10] of adding alloying elements like Nb and Ti have been done to get rid of the corrosion attack sites. That is because the added Ti to the austenitic stainless steel combines with the carbon in the matrix and forms TiC to increase the intergranular corrosion resistance, corrosion resistance at high temperature, and heat-resistance,[11] as well. Nb like Ti is also added to prevent the intergranular corrosion. In order that Nb may combine with the carbon, theoretically Nb of four times the carbon weight is enough, but actually five times is added in consideration of Nb combination with nitrogen, too. If Ti oxide, nitride and carbide forms in quantity during solidifying, the linear defects take place in process of hot rolling and cold rolling. To prevent the linear defects an appropriate Nb:C ratio is required.[12-13] According to those preceding studies, the carbon is an element which forms $M_{23}C_6$ and so Ti or Nb is added to form TiC or NbC prior to formation of $M_{23}C_6$. But, there are neither many studies about the microstructure change or intergranular corrosion depending on Nb content at time of the sensitizing treatment nor many reports on the welding conditions and comparison of heat treatment conditions.

In this study, after making alloy by adding Nb of 0.3 ~ 0.7 wt% to the austenitic stainless steel to make Nb:C ratio range of 4 ~ 11 with the purpose of improving the intergranular corrosion resistance of the stainless steel, fabricated austenitic stainless steel was investigated the mechanical properties and intergranular corrosion characteristics after solutionized and sensitized treatment, and compared intergranular corrosion at the welded zone, heat-affected zone, and the matrix.

## 2. Experimental

### 2.1. Preparation of the specimens

The specimens used in this experiment are AISI 304 stainless steel containing Nb content of 0.3 ~ 0.7 wt% melted in a vacuum. The melted steel was cast into 10 kg ingot, hot-rolled to 12 mm thickness at 1100℃, and had a solutionizing treatment. The hot-rolled steel was pickled to remove oxide scales and cut into the desired size of the specimen. The prepared specimens had the chemical composition shown in Table 1.

**Table 1. Chemical composition of samples**

| Alloy \ Elements (wt%) | C | Cr | Ni | Si | Mn | S | P | Nb | Fe | Nb/C |
|---|---|---|---|---|---|---|---|---|---|---|
| 12 | 0.065 | 19.03 | 9.340 | 0.863 | 1.730 | 0.019 | 0.032 | 0.290 | bal. | 4.46 |
| 13 | 0.066 | 18.94 | 9.400 | 0.871 | 1.720 | 0.020 | 0.033 | 0.464 | bal. | 7.03 |
| 14 | 0.065 | 18.87 | 9.230 | 0.842 | 1.700 | 0.022 | 0.029 | 0.718 | bal. | 11.04 |

### 2.2 The sensitized treatment and welding of the stainless steel

#### 2.2.1 Sensitized treatment of the specimens

The conditions of the heat treatment done to the specimens are shown in Table 2. The specimens were held for one hour in Ar gas of 1050℃ not to have precipitation of carbide and quenched in the water at 0℃. After a solutionizing treatment the specimens were kept in Ar gas at 650℃ for five hours to get precipitates intentionally and quenched in the water at 0℃ again for a sensitizing treatment. The specimens were numbered as shown in the table 2. 'SOL' stands for 'solutionizing treatment' and 'SEN' stands for 'sensitized treatment.' 0.3 or 0.7 mean the content of Nb contained in the stainless steel. XRD was used to make sure the metallurgical structure formed after heat treatment. X-ray target was Cu Kα(wave = 1.5405 Å).

**Table 2. The heat treatment condition of samples**

| Samples | Heat Treatments |
|---|---|
| SOL 0.3Nb | 1050℃, 1hr + 0℃, Water Cooling |
| SOL 0.5Nb | 1050℃, 1hr + 0℃, Water Cooling |
| SOL 0.7Nb | 1050℃, 1hr + 0℃, Water Cooling |
| SEN 0.3Nb | SOL + 650℃, 5hr + 0℃, Water Cooling |
| SEN 0.5Nb | SOL + 650℃, 5hr + 0℃, Water Cooling |
| SEN 0.7Nb | SOL + 650℃, 5hr + 0℃, Water Cooling |

#### 2.2.2 MIG welding of the specimens

The specimens after a solutionizing treatment were grooved with v-shape and welded face-to-face at the speed of 30 cm/min using the welding rods of 304 stainless steel with 25V and 300A. The protection gas was Ar gas with consumption of 15 ℓ/min. The micro-structure change of the welding point was observed using an optical microscope after electrolytic etching in 10% oxalic acid solution. The welded specimens were numbered 12, 13, and 14 depending on the Nb content of 0.3, 0.5, and 0.7 wt% respectively. The melted zone, the heat affected zone(HAZ), and the matrix were respectively marked 121, 122, and 123.

#### 2.2.3 Examination of mechanical properties of the specimens

To examine the mechanical properties of the specimens depending on the Nb content, the hardness and tensile strength were measured. The hardness of the solution-treated specimen was measured with Vickers hardness tester at the welded zone and HAZ with weight of 5 $kg/mm^2$. The specimen for tensile strength was cut parallel to the rolling direction and tensile strength was measured using Instron Model 6027 and the fractured surface after the test was examined with SEM.

#### 2.2.4 The test of the intergranular corrosion characteristics

Φ13 mm specimens were prepared to perform an intergranular corrosion test of the heat-treated and welded stainless steel. The test of intergranular corrosion extent on the different Nb content specimens was done in 10% oxalic acid solution with 2V for 5 minutes and the corrosion morphology was observed with SEM. The extent of intergranular corrosion of the surface was examined by an optical microscope and evaluated by an electrochemical method. Ar gas was continuously supplied to the electrochemical test solution of the cell to maintain deaerated atmosphere. For this test, the reference electrode was a saturated calomel electrode(SCE), counter electrode was high density carbon electrode, and the working electrode was the prepared specimen. DL-EPR(double loop electrochemical potentiokinetic reactivation: EG&G Co. 273A Potentiostat) method was used to investigate the degree of sensitization of the stainless steel and the intergranular corrosion characteristics of the welding zone with Nb content. The measurement was made by forward scan at a scanning speed of 100 mV/min. increasing up to 700 mV and again by reverse scan at the same scanning speed in the mixed solution of 0.1 M $H_2SO_4$ + 0.01 M KSCN for the heat-treated steel samples and in the mixed solution of 0.5M $H_2SO_4$ + 0.01M KSCN for the welded samples. The reactivation current density (Ir) was obtained from this curve. The effects of Nb content on the sensitization and the intergranular corrosion of the welding zone were compared. After EPR test, the surface morphologies were observed by SEM for intergranular corrosion behavior.

## 3. Results and discussion

### 3.1 Nb content effects on the microstructure and the crystalline structure

Fig. 1 is the photos of the microstructure for the solution-treated and sensitized specimen in order to examine the effect of Nb. (a), (b), (c), and (d) are SOL0.3Nb, SOL0.7Nb, SEN0.3Nb, and SEN0.7Nb respectively. In comparison of (a) and (c) which have the same content of 0.3 wt% Nb, the solution-treated (a) has little intergranular corrosion and has twin boundary formed during heat treatment, but the sensitized (c) has the corrosion morphology of intergranular attacked CDZ (chromium depleted zone), due to precipitation of chrome carbide, which hints the presence of intergranular precipitates. (b) and (d) photos hardly show any intergranular corrosion. Especially, (d) does not have intergranular corrosion even in oxalic acid solution in spite of sensitizing treatment. It is thought that the added Nb made the carbon precipitated in the grain boundaries as NbC and suppressed

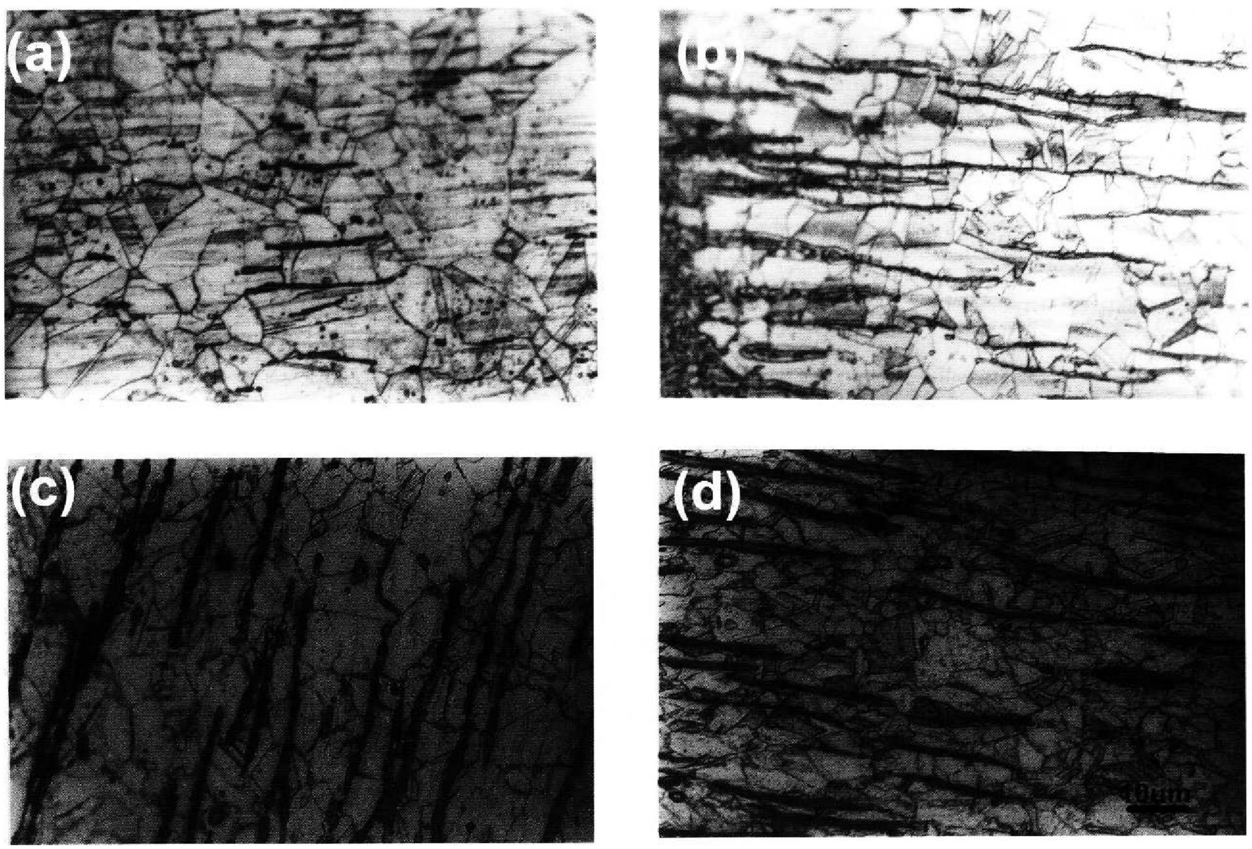

**Fig. 1.** Optical micrographs of SOL0.3Nb(a), SOL0.7Nb(b), SEN0.3Nb(c) SEN0.7Nb(d) after etching in 10% oxalic acid.

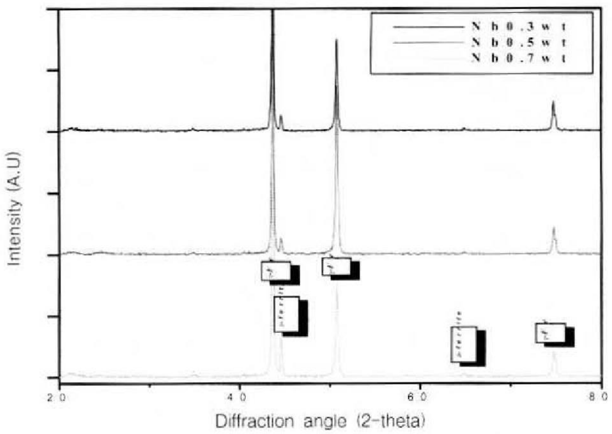


**Fig. 2.** X-ray diffraction patterns of the solutionized stainless steels containing Nb.

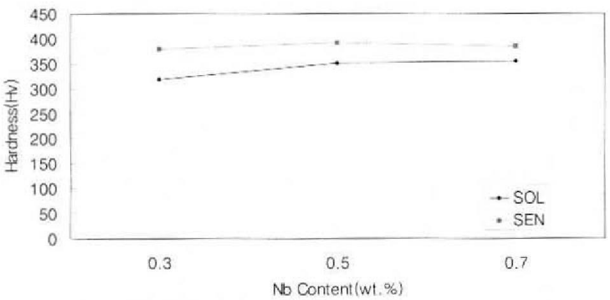


**Fig. 3.** Hardness of the solutionized and sensitized stainless steels as function of Nb content.

formation of $M_{23}C_6$[14]. Also, in (b) and (d) which have more Nb than in (a) and (c), more second phases are observed. This is in accordance with the report that Nb is a powerful element which forms second phases. This is also proved by the fact that XRD result of Fig. 2 for low Nb content mostly has same peak as in austenitic stainless steel, but Nb content of 0.7 wt% has sure δ-ferrite peak.

### 3.2 Nb effects on the mechanical properties of the sensitized specimen

Fig. 3 is the hardness variation with Nb content of the solution-treated and sensitized 304 stainless steel. In the case of the sensitized steel, higher Nb content showed tendency of slightly increasing hardness. The increased hardness seems to be the result that δ-ferrite precipitated by the added Nb worked as a reinforcing agent.[15] Especially, the sensitized case had slightly higher hardness than the solution-treated one. It is thought that the carbide like NbC was precipitated inside the granule and resulted in reinforcement together with the reinforcing effect of δ-ferrite.

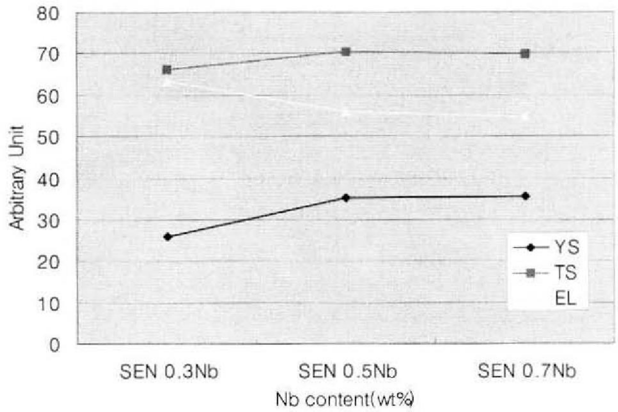


**Fig. 4.** Results of tensile test of the sensitized stainless steels.

Fig. 4 is a diagram of change of the mechanical properties (tensile strength, yield point, and elongation) of the sensitized and solution-treated 304 stainless steel with Nb content. The tensile strength was similar both in solution-treated steel and sensitized steel and did not change greatly depending on Nb content variation. The tensile strength of the solution-treated steel slightly decreased as a result that the stretched δ-phase worked as propagation route of the cracks at γ/δ boundaries.[16] However, the tensile strength of the sensitized steel increased from Nb content of 0.5 wt%. It is thought that it was because the effect of precipitation hardening by NbC carbide was greater than the tensile strength decrease by δ-ferrite, as previously studied. The yield strength and elongation had same tendency as the tensile strength, and so the elongation of 0.3 wt%Nb specimen was higher than that of 0.7 wt%Nb specimen.

Fig. 5 is the photos of the fractured surface observed by SEM after tensile strength test of the solution-treated and sensitized specimens of varied Nb content. In the case of solution-treated specimens, the cracks took place at the γ/δ boundaries by the increased δ-ferrite as Nb content increases, as shown in the photos (a) 0.3 wt%Nb, (b) 0.5 wt%Nb, and (c) 0.7 wt%Nb. The photos (d), (e), and (f) are the sensitized specimens of 0.3 wt%Nb, 0.5 wt%Nb, and 0.7 wt%Nb respectively. In those photos the cracks show intergranular break. It means there are second phase like the intergranular precipitates or impurities. Those photos also show the dimple fracture appearance, and so it conforms to the characteristics of the tensile strength, yield strength, and elongation shown in Fig. 4.

### 3.3 Intergranular corrosion characteristics of the sensitized stainless steel

Fig. 6 is the photos observed by SEM after intergranular corrosion test in 10% oxalic acid solution to investigate

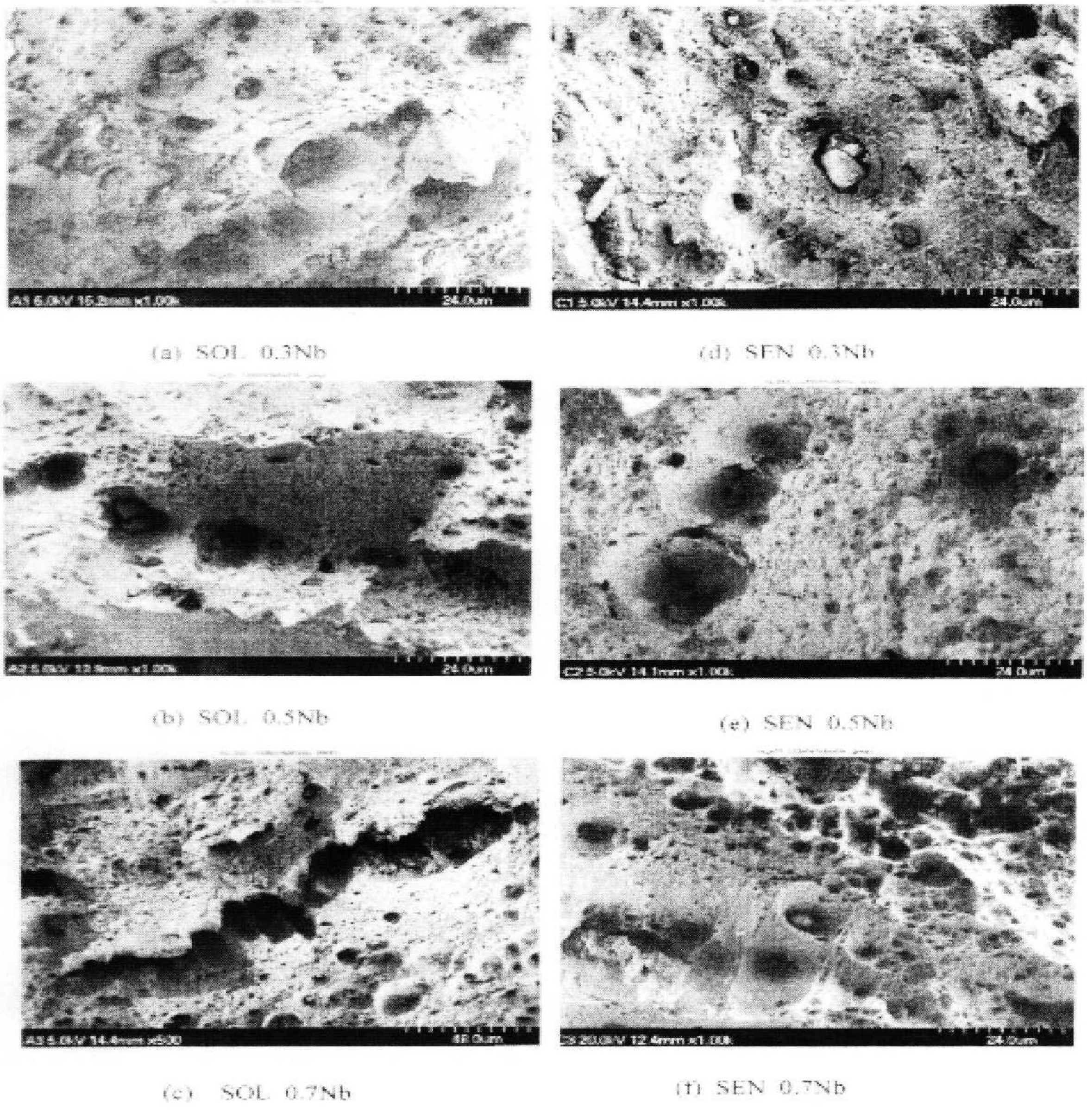


**Fig. 5.** SEM fractographs of the solutionized(a,b,c) and sensitized (d,e,f) stainless steels containing Nb after tensile test.

the effect of Nb content. As shown in the solution-treated specimens of 0.3 wt%Nb(a), 0.5 wt%Nb(b) and 0.7 wt%Nb(c), δ-ferrite formation increases as Nb content goes up, but the intergranular corrosion is not observed at γ/δ boundary. But, the sensitized specimens of 0.3 wt%Nb(d), 0.5 wt%Nb(e), and 0.7 wt%Nb had severe intergranular corrosion. That is because the corrosion starts around the precipitated phase at the early stage due to NbC precipitation at γ/δ boundary and finally δ-ferrite phase is corroded. It is found that (e) and (f) with more Nb content show notably decreased intergranular corrosion.

Fig. 7 is EPR curve measured in the solution of 0.1M $H_2SO_4$ + 0.01M KSCN on the solution-treated specimens and the sensitized ones of varied Nb content. The solution-treated specimens have tendency that the activation current density(Ia) and the reactivation current density(Ir) slightly increase as Nb content goes up. That is because Nb addition sufficiently provided the space where SCN- ion precipitates as δ-ferrite amount increases. In the meantime, the sensitized specimens show almost same Ia though Nb content increases,[17] but it proves that the effect of Nb

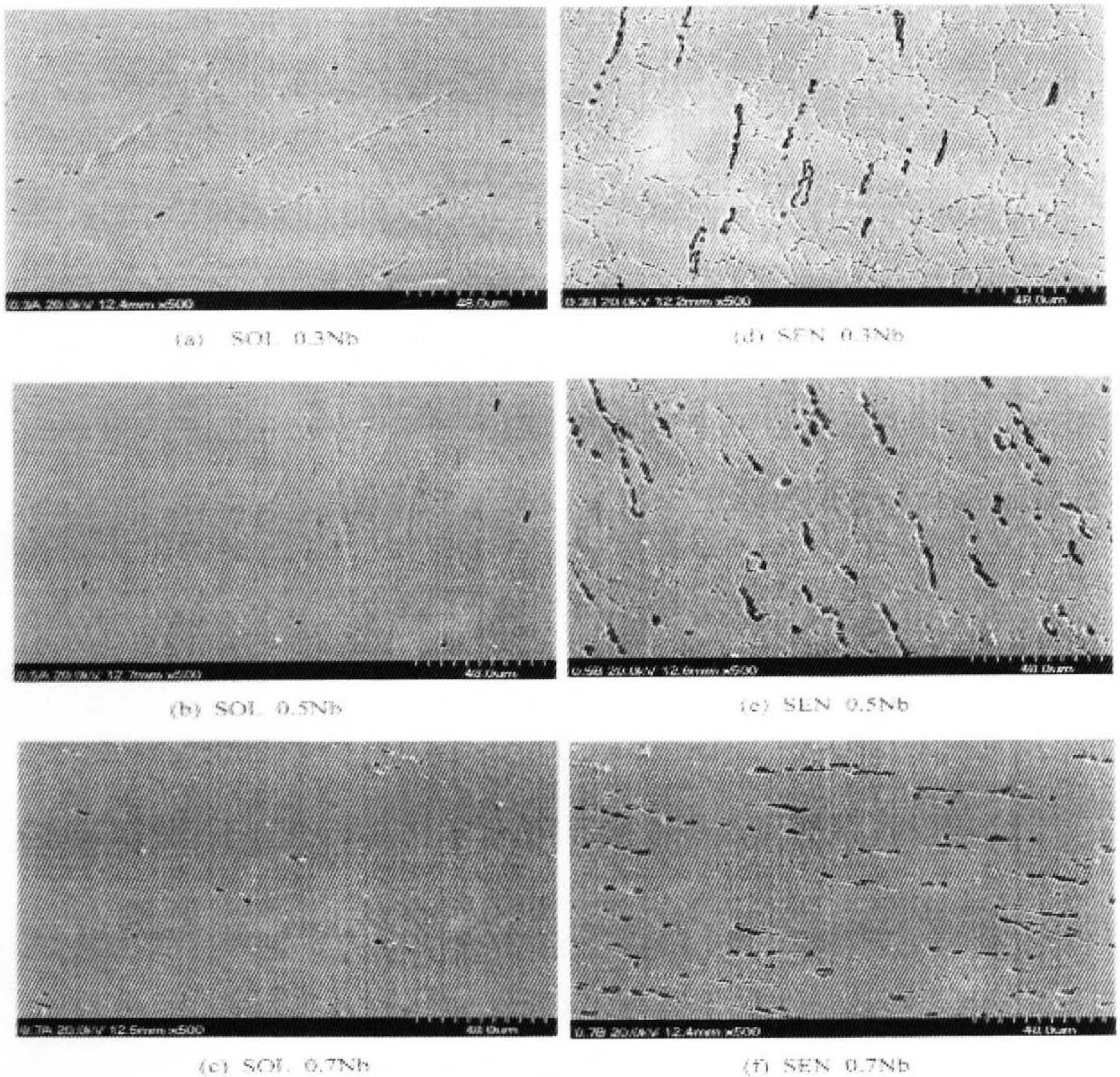


**Fig. 6.** SEM micrographs showing intergranular corrosion of the solutionized(a,b,c) and sensitized (d,e,f) stainless steels containing Nb after corrosion test in oxalic acid.

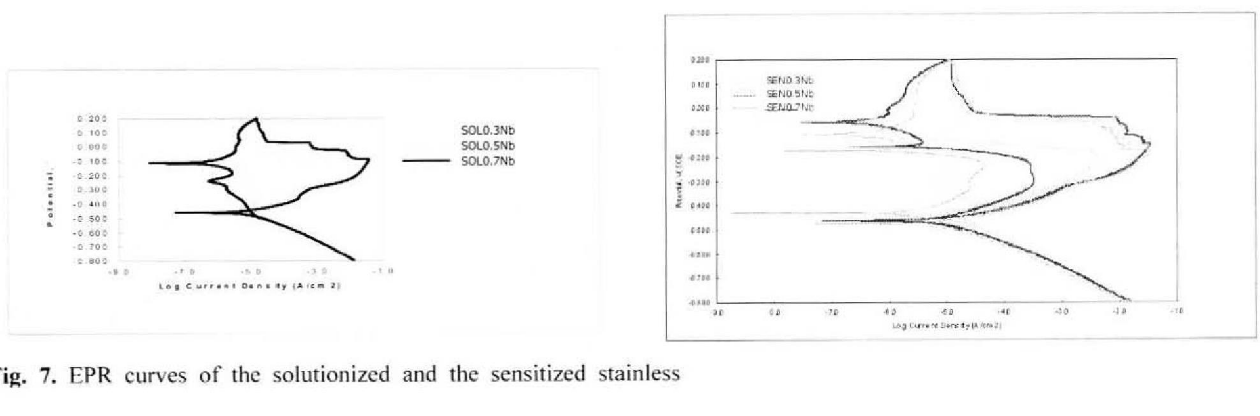


**Fig. 7.** EPR curves of the solutionized and the sensitized stainless

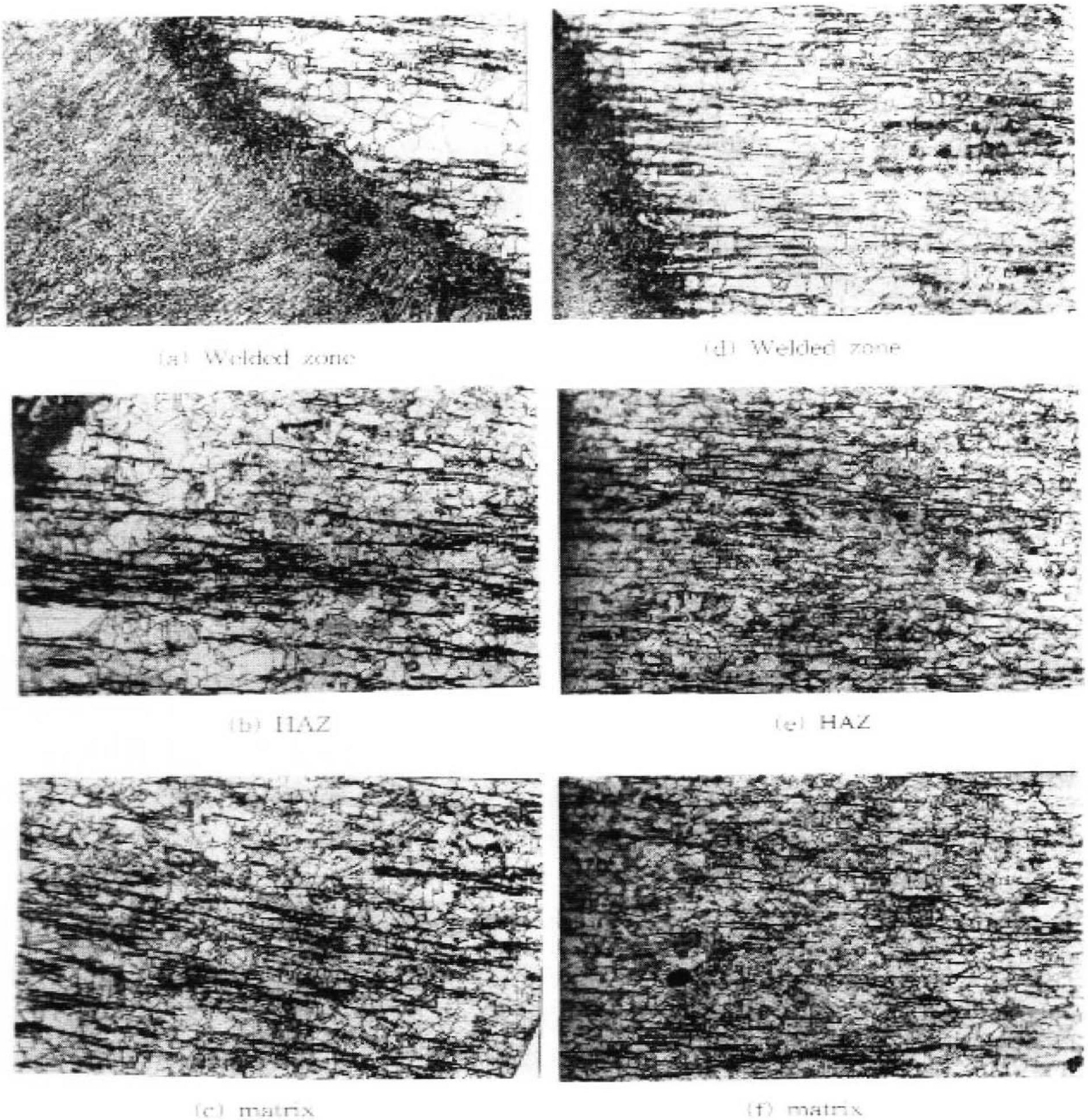


**Fig. 8.** Optical micrographs of welded stainless steels containing 0.3 wt%(a, b, c) and 0.5 wt%(d, e, f) Nb after etching in 10% oxalic acid.

addition remarkably appears from the fact that Ir difference is in the range of $10^{-2}$ A/cm$^2$ to $10^{-4}$ A/cm$^2$ and the difference is as low as 1~2 order.

### 3.4 Microstructure and crystalline structure of the welding zone with Nb content

Fig. 8 is the micrographs of the specimens taken from the melted zone, the heat-affected zone, and the matrix to investigate the Nb effect given to the microstructure of the welding zone. At (a) corresponding to the melted zone of 0.3 wt%Nb specimen, dendritic structure, which is mainly mixture of austenitic shapes and δ-ferrite shapes, is observed.[18] Brown[19] and others reported that the melted metal structure appears as the mixed structure of γ/δ and δ-ferrite forms up to 16% when 304 and 316 stainless steel are welded. Also in this study it is found that δ-ferrite is formed in quantity at the melted metal zone and crystalline grains are shown at the matrix in its vicinity differently from the melted zone. (b) is a structure corresponding to HAZ, which has the precipitates at grain

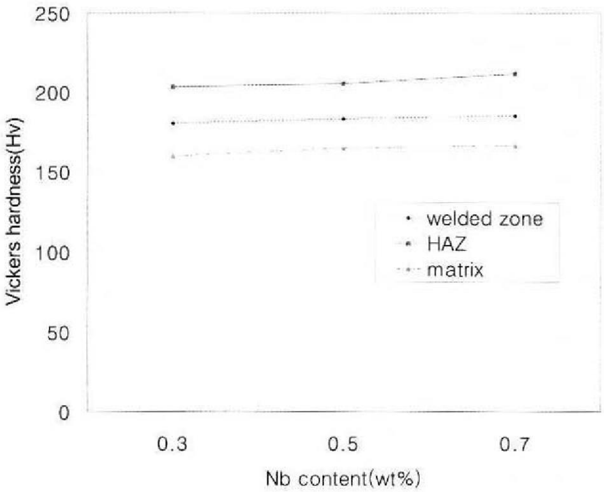


**Fig. 9.** Micro-vickers hardness of welded zone, HAZ, and matrix for stainless steels as function of Nb content.

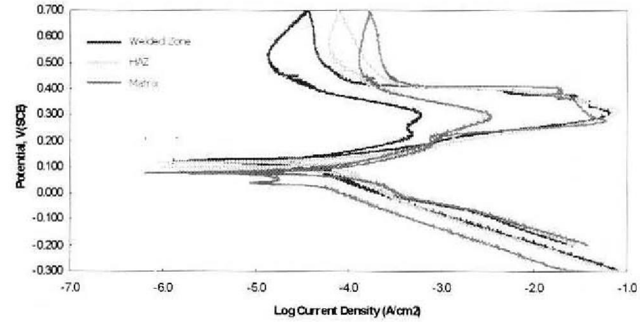


**Fig. 10.** EPR curves for the welded zone, HAZ, and the matrix of stainless steels containing 0.3 wt% Nb in 0.1M $H_2SO_4$ + 0.01M KSCN solution at 25℃.

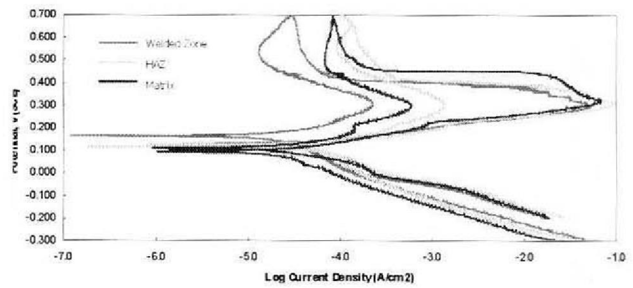


**Fig. 11.** EPR curves for the welded zone, HAZ, and the matrix of stainless steels containing 0.5 wt% Nb in 0.1M $H_2SO_4$ + 0.01M KSCN solution at 25℃.

boundaries, and it proves that there are many twin boundaries which show up when the austenitic structure is heat-affected. (c) is a photo of the matrix. It does not steels in 0.1 M $H_2SO_4$ + 0.01 M KSCN solution at 25℃. show the formation of the precipitates. (d) of 0.5 wt%Nb content has more δ-ferrite formed at the melted zone. By Nb effect at the HAZ, $M_{23}C_6$ precipitates do not appear differently as in (b), but it is found that merely δ-ferrite amount increased. The matrix shows similar aspect.

Fig. 9 is the result measured by Vickers hardness tester to investigate the hardness change at the melted zone, HAZ, and the matrix by Nb content increase. The hardness increases in the order of HAZ, the melted zone, and the matrix. It also shows a tendency of slightly increasing hardness as Nb content goes up. It seems to be a similar aspect to the sensitized case and it is thought that δ-ferrite formed by Nb addition functioned as a reinforcing agent.[15]

### 3.5 Intergranular corrosion characteristics of the welded zone with Nb content

Fig. 10 is EPR curve, of the 0.3 wt%Nb specimens taken from the melted zone, HAZ, and the matrix, measured in the solution of 0.5 M $H_2SO_4$ + 0.01 M KSCN to investigate Nb effect given to the intergranular corrosion of the welding zone. From Ir value of the melted zone, HAZ and the matrix, 0.3 wt%Nb has superior intergranular corrosion resistance. The highest Ir at HAZ proves that there are the precipitates formed at that zone.

Fig. 11 is EPR curve of the melted zone, HAZ, and the matrix, measured in the solution of 0.5M $H_2SO_4$ + 0.01 M KSCN, with Nb content increased to 0.5 wt%. In this case, less Ir is found at the melted zone, HAZ, and the matrix than in 0.3 wt%Nb. Especially Ir greatly decreased at HAZ and it is understood that Nb restrained Nb or Cr carbide formation. Also, in the case of the specimens of same Nb content, Ir values of the melted zone and the matrix are lower than that of HAZ. It is thought that Ir became higher since corrosion resistance was lowered by NbC formation, though Nb restrains the corrosion since the intergranular corrosion takes place along the carbide precipitates spot by the lowered Cr amount caused by formation of $Cr_{23}C_6$ carbide at the austenitic phase formed near γ/δ boundary though δ-ferrite forms by Nb addition.[20] Also, there is a report[21] that corrosion resistance decrease if δ-ferrite phase increases. That is the case of $Cr_{23}C_6$ carbide formation along δ-ferrite phase when sensitized. In this study, however, it is understood that the superior corrosion resistance is shown at the melted zone and the matrix since Nb is contained.

Fig. 12 is EPR curve of the melted zone, HAZ, and the matrix of 0.7 wt%Nb measured in the solution of 0.5 M $H_2SO_4$ + 0.01 M KSCN. Here, Ir and the current density of passive region drastically decrease when Nb content is increased to 0.7 wt%. Table 3 shows the degree of

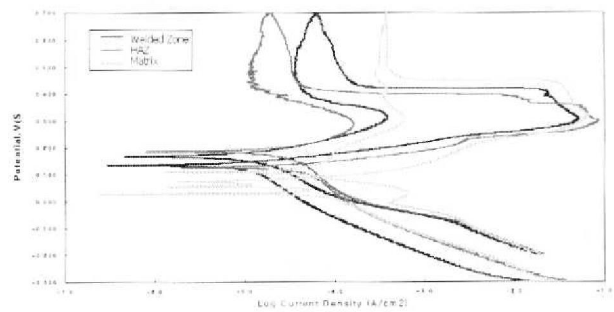


**Fig. 12.** EPR curves for the welded zone, HAZ, and the matrix of stainless steels containing 0.7 wt% Nb in 0.1M $H_2SO_4$ + 0.01M KSCN solution at 25℃.

**Table 3. Degree of Sensitization of samples**

| Nb Content (wt%) | Degree of Sensitization(Ir/Ia × 100%) | | |
|---|---|---|---|
| | Welded Zone | HAZ | Matrix |
| 0.3 | 1.001 | 3.333 | 1.555 |
| 0.5 | 0.833 | 1.111 | 0.875 |
| 0.7 | 0.500 | 0.522 | 0.750 |

sensitization of samples. The fact observed by Fig. 10 is reassured by this. Fig. 13 is SEM photos of the corroded surface, taken after EPR test in the solution of 0.5 M $H_2SO_4$ + 0.01M KSCN, of the melted zone, HAZ and

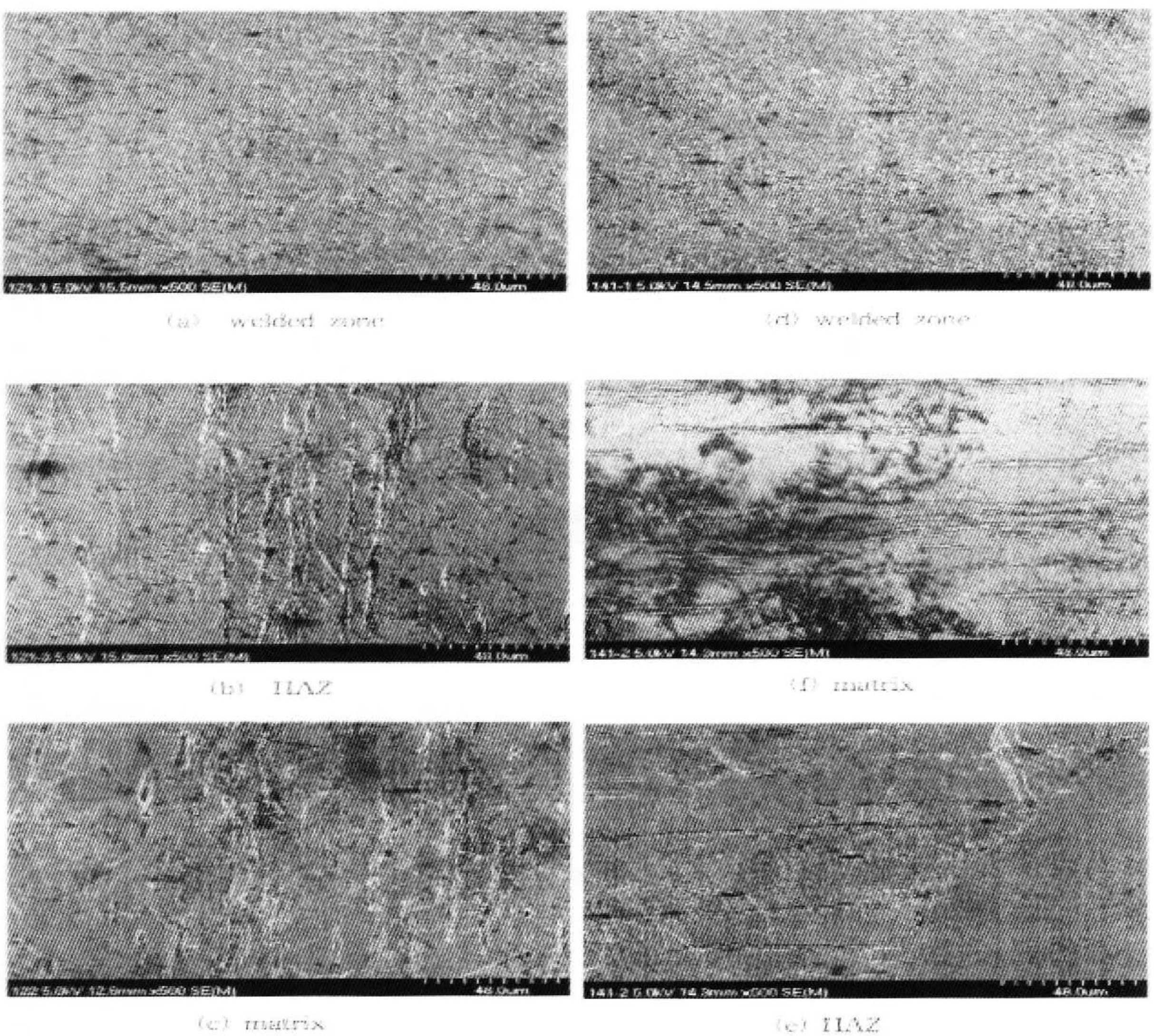


**Fig. 13.** SEM micrographs showing the intergranular corrosion of welded stainless stainless steels containing 0.3 wt%(a,b,c) and 0.7 wt%(d,e,f) Nb after EPR test in 0.1M $H_2SO_4$ + 0.01M KSCN solution at 25℃.

the matrix of 0.3 wt%Nb and 0.7 wt%Nb specimens to investigate Nb effect given to the intergranular corrosion of the welded zone. (a), (b), and (c) are the photos of specimen 12 at the melted zone, HAZ, and the matrix. (d), (e), and (f) are the photos of specimen 14 at the melted zone, HAZ, and the matrix. (a) has almost no δ-ferrite corrosion. (b) shows δ-ferrite phase corrosion and the intergranular corrosion by SCN- at the spot where the carbide seems to be precipitated. (c) also shows corrosion at the place where δ-ferrite phase existed, but the intergranular corrosion is not shown. Also, it is proved in (d), (e), and (f) that the intergranular corrosion decreases as Nb content increases. The corrosion aspect of the specimen with Nb increased to 0.7 wt% is well in accordance with EPR curve and it assures the excellent corrosion resistance of 0.7 wt%Nb specimen.

## 4. Conclusions

1) 304 stainless steel with lower Nb content has mainly austenitic structure, but with 0.7 wt% Nb content δ-ferrite structure clearly appears. The more Nb content, the harder the sensitized steel is. The tensile strength and yield strength increase in the specimens with 0.5 wt% Nb content or more. Elongation is highest at 0.3 wt%Nb specimen and lowest at 0.7 wt%Nb specimen.

2) As a result of intergranular corrosion test performed in 10% oxalic acid solution, the solution-treated specimens have deeper intergranular corrosion as Nb content increases, while the sensitized ones have a tendency of less intergranular corrosion. The sensitized specimens tested in the solution of 0.1 M $H_2SO_4$ + 0.01M KSCN have almost same Ia and drastically decreasing Ir as Nb content increases.

3) The melted zone is a dendritic structure constituted of austenitic phase and δ-ferritic phase. As Nb content decreases, the precipitates forms between the heat-affected grains and twin boundary appears, but the precipitates was not formed at the matrix. The hardness of the welding zone increases in the order of HAZ, the melted zone, and the matrix. The higher Nb content showed the harder the hardness.

4) As Nb content increases, from EPR curve Ir and Ia greatly decrease in the order of the melted zone, the matrix, and HAZ. And severe intergranular corrosion takes place at HAZ.

## Acknowledgement

This study was financially supported by Chonnam National University year of 2000

## References

1. H. H. Uhlig and R. A. White, *Trans.*, ASM, **56**, 866 (1956).
2. S. Barnartt and D. Van Rooyzn, *J. Electrochem.. Soc.*, **109**, 343 (1962).
3. S. Szklarska-Smialowska and G. Cragnolino, *Corros.*, **36**, 653 (1980).
4. P. L. Andresen, *Corros.*, **38**, 53 (1982).
5. E. C. Bain, R. H. Aborn, and J. J. B Rutherford, *Trans. Amer. Soc. Steel Treat.*, **21**, 481 (1933).
6. I. Olefjord and Bengt-Olef Elfstom, *Corros.*, **38**, 46 (1982).
7. H. C. Choe and K. H. Kim, *J. Corros. Sci. Soc. of Korea*, **21**, 31 (1992).
8. B. E. Wilde, C. D. Kim, and J. C. Turn JR., *Corros.*, **38**, 515 (1982).
9. D. Itzhak and S. Harush, *Corros. Sci.*, **25**, 883 (1985).
10. S. Lal and G. S. Upadhyaya, *J. Mater. Sci.*, **24**, 3069 (1989).
11. D. M. Follstaedt, F. G. Yost, L. E. Pope, S. T. Picraux, and J. A. Knapp, *Appl. Phys. Lett.*, **43**, 358 (1983).
12. V. Ciahl, *Prot. Met.(USSR)*, **4**, 563 (1968).
13. R. Stricker, *Trans. ASM*, **54**, 362 (1961).
14. S. O. Cha, H. C. Choe, and K. H. Kim, *J. of the Korean Inst. of Met & Mater.*, **36**, 138 (1998).
15. Y. Iwabuchi, *Materials Transactions, JIM*, **33**, 627 (1992).
16. G. Sui, E. A. Charles, and J. Congleton, *Corros. Sci.*, **38**, 687 (1996).
17. H. C. Choe and K. H. Kim, *J. of the Korean Inst. of Met & Mater.*, **29**, 979 (1991).
18. H. Nakamura, *J. Welding, Japan*, **3**, 48 (1985).
19. R. Brown, *J. Materials for Energy Systems*, **7**, 55 (1985).
20. V. Cihal, *Trans. ISIJ*, **25**, 419 (1985).
21. C. J. Newton, *Mat. Sci. Tech.*, **2**, 181 (1986).